



UNIVERSITY OF LEEDS

This is a repository copy of *Lift-off and blow-off of methane and propane subsonic vertical jet flames, with and without diluent air*.

White Rose Research Online URL for this paper:  
<http://eprints.whiterose.ac.uk/102104/>

Version: Accepted Version

---

**Article:**

Palacios, A, Bradley, D and Hu, L (2016) Lift-off and blow-off of methane and propane subsonic vertical jet flames, with and without diluent air. *Fuel*, 183. pp. 414-419. ISSN 0016-2361

<https://doi.org/10.1016/j.fuel.2016.06.073>

---

© 2016. This manuscript version is made available under the CC-BY-NC-ND 4.0 license  
<http://creativecommons.org/licenses/by-nc-nd/4.0/>

**Reuse**

Unless indicated otherwise, fulltext items are protected by copyright with all rights reserved. The copyright exception in section 29 of the Copyright, Designs and Patents Act 1988 allows the making of a single copy solely for the purpose of non-commercial research or private study within the limits of fair dealing. The publisher or other rights-holder may allow further reproduction and re-use of this version - refer to the White Rose Research Online record for this item. Where records identify the publisher as the copyright holder, users can verify any specific terms of use on the publisher's website.

**Takedown**

If you consider content in White Rose Research Online to be in breach of UK law, please notify us by emailing [eprints@whiterose.ac.uk](mailto:eprints@whiterose.ac.uk) including the URL of the record and the reason for the withdrawal request.



[eprints@whiterose.ac.uk](mailto:eprints@whiterose.ac.uk)  
<https://eprints.whiterose.ac.uk/>

# **Lift-Off and Blow-Off of Methane and Propane Subsonic Vertical Jet Flames, With and Without Diluent Air**

**Palacios, A.,<sup>1\*</sup> Bradley, D.,<sup>2</sup> Hu, L.<sup>3</sup>**

<sup>1</sup>Universidad de las Americas, Puebla, Department of Chemical, Food and Environmental Engineering,  
Puebla 72810, Mexico.

<sup>2</sup>University of Leeds, School of Mechanical Engineering, Leeds LS2 9JT, UK.

<sup>3</sup>University of Science and Technology of China, State Key Laboratory of Fire Science, Hefei, Anhui  
230026, China.

\*Corresponding author. E-mail address: [adriana.palacios@udlap.mx](mailto:adriana.palacios@udlap.mx)

## Abstract

The paper seeks to increase understanding of subsonic jet flame blow-off phenomena, through experimental studies that include the controlled introduction of air into the fuel jet. As the molar concentration of air in the jet flame gas,  $A_j$ , is increased the reaction zone becomes leaner, and the flame lift-off distance increases. Eventually, flame oscillations develop and are followed by flame blow-off. A jet mixing analysis enables the extent of the leaning-off of the mixture to be estimated. From this, the reduced mean flamelet burning velocity,  $u_a$ , is found at the location of the pure fuel jet flame. The conditions for blow-off are correlated with the last measured stable values of the dimensionless flow number,  $U_b^*$ , for methane and propane jet flames, with and without added air. Values of  $U_b^*$  decline as the proportion of added air increases, more markedly so with methane. This is attributed to the leaning-off of the flame, and the associated decrease in the flame extinction stretch rate. As  $U_b^*$  declines in value, with increasing air dilution, the emissions of unburned hydrocarbons just prior to blow-off increase. An underlying generality of the findings is revealed when  $u_a$  is introduced into the expression for  $U_b^*$ , and  $A_j$  is normalised by the moles of air required to burn a mole of fuel.

## Nomenclature

$A_j$	mole fraction of air in jet flow
$D$	internal pipe diameter (m)
$f$	ratio of fuel to air moles in stoichiometric fuel-air mixture
$F_j$	mole fraction of fuel in jet flow
$(F/A)_j$	ratio $F_j/A_j$
$(F/A)_s$	ratio $F_j/A_j$ for required near-stoichiometric conditions
$L$	lift-off distance (m)
$P_a$	pressure of the ambient atmosphere (MPa)
$P_i$	initial stagnation pressure (MPa)
$r$	flame radius (mm)
$S_L$	maximum laminar burning velocity of the mixture under ambient conditions (m/s)
$t$	time (s)
$u$	pipe flow mean exit velocity, or sonic velocity for choked flow (m/s)
$u_a$	flamelet burning velocity for aerated jet flame at location of $\phi_m$ contour of non-aerated jet flame (m/s)

- $U^*$  dimensionless flow number,  $U^* = (u/S_L)(D/\delta)^{-0.4}(P_i/P_a)$ .
- $U_b^*$  dimensionless  $U^*$  flow number just prior to blow-off conditions
- $U_{ba}^*$  dimensionless  $U_b^*$  flow number based on  $u_a$
- $U_{bo}^*$  dimensionless  $U_b^*$  flow number at  $A_j = 0$ ,  $U_{bo}^* = U_b^*$  at  $A_j = 0$ .

### Greek symbols

- $\delta$  laminar flame thickness under ambient conditions (m), given by  $\nu/S_L$
- $\phi_a$  aerated jet equivalence ratio
- $\phi_j$  equivalence ratio of aerated jet in supply pipe
- $\phi_m$  equivalence ratio for non-aerated fuel jet flame remote from blow-off
- $\nu$  gaseous mixture kinematic viscosity at ambient conditions corresponding to those for  $S_L$  ( $m^2/s$ )

### Subscripts

- j jet gas mixture
- s stoichiometric, or required near-stoichiometric conditions

**Keywords:** Jet flame; Blow-off; Lift-off; Burning velocity; Air-diluted jet flames; Jet mixing.

## 1. Introduction

It is important to be able to predict flame lift-off distances, plume heights, and blow-off conditions, of steady jet flames on a burner, in both controlled flaring and the jet flames that follow unintended explosive blow-outs. Such flames become unstable at both low and high jet velocities, the latter ultimately leading to flame blow-off. In controlled flaring, cross winds, fuel dilution, and fluctuations in flow rate can all result in incomplete combustion, flame extinction, and blow-off. Yet high combustion efficiencies are essential in, for example, the flaring associated with hydraulic fracturing to liberate methane, in order to prevent the uncontrolled release of this potent greenhouse gas. Johnson and Kostiuk [1] have shown that the addition of diluents, such as  $N_2$  and  $CO_2$ , in sufficient proportions seriously reduces the combustion efficiency. Ingress of air into naturally occurring methane is less well understood, in this regard, as is also the extent to which flare performance might be impaired by flame blow-off at a lower jet velocity. The present paper reports an experimental study of the effect on the blow-off velocity of a subsonic jet of adding air to, respectively,

methane and propane fuel jets. In so far as the addition of air aids fuel/air mixing, higher jet velocities might be expected before blow-off occurs. On the other hand, excess air might induce earlier lean flame extinction and blow-off.

There have been significant successes in the mathematical modelling of lift-off distances,  $L$ , and plume heights for pure fuel jet flames, and in the associated formulation of appropriate dimensionless groups for the correlation of experimental data [2-6]. The region between the exit plane of a fuel jet discharging into the atmosphere and the flame leading edge is one of intense mixing that generates high strain rates. This is illustrated in Fig. 1, derived from the computations reported in [3]. The dashed curves show radial and axial changes in the streamlines, and the full line contours show the mean volumetric heat release rate. The strain rates are initially sufficiently high to not only effectively mix the fuel and surrounding air, but also to exceed the flame extinction stretch rates, and quench any potential flamelets. Further downstream the strain rates relax to the extent that combustion becomes possible in the most reactive flamelets, which also have the highest flame extinction stretch rates, and a laminar burning velocity close to  $S_L$ .

With further increases in jet velocity, more air is entrained, localised equivalence ratios fall as the mixture leans off, and flame extinction stretch rates decrease, to the extent that eventually all flamelets are extinguished and the flame blows off. Computations of the distributions of equivalence ratios show that at flow velocities, before approaching blow-off, the peak value in probability density function is close to that for the maximum burning velocity of the mixture. This supports the widespread use of the maximum value of the laminar burning velocity of the mixture,  $S_L$ , in dimensionless groups for correlating lift-off distance and blow-off [6,7].

The stretched laminar flamelet modelling in [2-4], in conjunction with experimental jet flame data, have led to more practical, generalised, correlations of experimental jet flame data, involving a dimensionless flow number,  $U^*$ , that is closely related to the Karlovitz stretch factor, employed in premixed turbulent combustion [6], where

$$U^* = (u/S_L)(D/\delta)^{-0.4}(P_i/P_a). \quad (1)$$

A normalised flame lift-off distance,  $(L/D)_f$ , was expressed as a function of  $U^*$  by:

$$(L/D)_f = 0.1U^* - 0.2, \text{ for subsonic jets.} \quad (2)$$

Here  $u$  is the pipe flow mean velocity (or sonic velocity for choked flow),  $\delta$ , the laminar flame thickness, at the ambient conditions, given by  $\nu/S_L$ , with  $\nu$  the gaseous mixture kinematic viscosity.  $P_a$  is the pressure of

the ambient atmosphere,  $P_i$  the initial stagnation pressure,  $D$ , the internal pipe diameter, and  $f$  the ratio of fuel to air moles in the stoichiometric fuel-air mixture, which is close to that for the maximum laminar burning velocity of the mixture,  $S_L$ . Extensive correlations of flame plume height and  $(L/D)f$  in terms of  $U^*$ , appear in [6].

However, the prediction of blow-off, as the ultimate limiting condition of lift-off, when localised extinctions cause the flame to simultaneously leave the burner and extinguish, presents more severe modelling problems [5]. They include the development of oscillatory, non-linear phenomena. Because of these complexities it is difficult to formulate correlations of blow-off in a generalised way. No attempt was made to correlate blow-off parameters in [6], while in [8] separate stable values of  $U^*$  prior to blow-off,  $U_b^*$ , are presented for six different jet fuels. Indeed, even lift-off distances could not be fully correlated in a general sense. Figure 2 shows the best overall correlation from 16 sources taken from [6], with inner diameters ranging between 0.84 and 51 mm, alongside the best separate correlations for  $C_3H_8$  and  $CH_4$  jets. Published data on blow-off are more sparse. For the relationship between lift-off distance and  $U^*$ , shown in Fig. 2, the pure fuel jet flames were stable from  $U^* = 5$  to higher values just prior to blow-off. Mathematical modelling in [3] shows that as  $U^*$  increases, more air is entrained and mixed with the fuel. Combustion then occurs in leaner flamelets. Further leaning-off with increasing  $U^*$  leads to flame stretch extinctions, and eventual blow-off.

With regard to the influence of added air to the fuel jet, values of  $U_b^*$  for each fuel and its added air can only be found for each mixture separately. Furthermore, there is no stabilised blow-off height, due to the very rapid rate of change in lift-off distance, and development of oscillations, as blow-off occurs. The procedure therefore adopted was to measure the key parameters, for aerated methane and propane jets, at the onset of the rapid increase in lift-off distance just prior to flame blow-off and derive a stable  $U_b^*$  from these readings.

Lift-off distances and  $U_b^*$  were measured as a function of the mole fraction of added air in the jet gas mixture,  $A_j$ . Eventually, sufficient added air induced earlier blow-off. Values of  $U_b^*$ , just prior to blow-off, fell sharply with increasing  $A_j$ . For propane these values ranged from about 60 with no dilution to about 10 with a mole fraction of air in the jet of 0.6. The findings are interpreted in terms of the understandings obtained from both the stable flame computational studies and also from a simple mixing theory, presented in Section 3, involving values of aerated fuel laminar burning velocities.

## **2. Measurements of Lift-Off and Blow-Off in Jet Flames**

Cylindrical stainless steel pipes, with inner diameters between 3 and 8 mm were employed for the jet flames, with supply lines from either a methane or propane cylinder, and added air. These diameters were within the range that was well correlated by the dimensionless groups in [6], such as the correlation in Fig. 2. Calibrated rotameters measured the separate flow rates before mixing, followed by flow into the jet pipe, and release into an atmosphere of still air at 0.1 MPa in the Hefei laboratory. This provided a configuration for measuring lift-off distance and observing instabilities of both pure fuel and air-diluted jet flames. Mass flow rates were calculated from flowmeter measurements. Visualisations of the jet flame details were by means of a digital Charge-Coupled Device, CCD, camera of sensor size 8.5 mm, with  $3.10^6$  pixels, operating at 25 frames per second.

Flame images were converted first to a grey scale, then a binary image. Batches of 1,000 consecutive images were converted to binary images for statistical analysis. Flame intermittency distributions were obtained by averaging the values of these consecutive binary images in each pixel position [9].

Results are expressed in terms of  $A_j$ , the mole fraction of air in the jet flow. If  $A_j$  and  $F_j$  and  $A_j$  are the fractional moles of air and fuel in one mole of jet gas mixture, their ratio,  $(F/A)_j$ , in the supply pipe is related to the equivalence ratio there,  $\phi_j$ , by  $(F/A)_j = \phi_j (F/A)_s$ , where  $(F/A)_s$  is the stoichiometric ratio with  $F_j + A_j = 1.0$ , then:

$$F_j = [1 + (A/F)_j]^{-1} = [1 + \phi_j^{-1}(F/A)_s^{-1}]^{-1}, \text{ and } A_j = [1 + (F/A)_j]^{-1} = [1 + \phi_j (F/A)_s]^{-1}. \quad (3)$$

Table 1 summarises the overall experimental conditions. Three sets of reading were taken for each condition to yield average values. Table 2 gives the values of the principal parameters associated with the evaluation of  $U_b^*$ . Methane/air oscillatory jet flame images, at intervals of 3 s, are shown in Fig. 3, and amplitudes of the unsteady oscillations as they developed just prior to blow-off, in Fig. 4. It can be seen how amplitudes increase and culminate in blow-off.

Typical measured values of  $(L/D)_f$ , leading to blow-off, are plotted against the mole fraction of air in the jet,  $A_j$ , in Figs. 5 and 6. Figure 5 shows some typical relationships for  $U^* = 10.7$  and  $13.2$  for methane/air jets, and Fig. 6 for  $U^* = 16.2$ , at higher  $A_j$ , for propane/air jets. Initially, for both fuels, the substitution of relatively small amounts of fuel by air had little effect on lift-off distances. Further substitution was followed by a steady increase in  $(L/D)_f$ , and eventual oscillations, followed by rapid blow-off. Values of  $U_b^*$  decreased as those of  $A_j$  were increased.

Table 2 gives the conditions for blow-off at different  $A_j$  for the dilution of both fuels, with the measured values of  $U_b^*$ . Data on the blow-off of pure fuel jet flames are sparse, but some are available from recent experiments in Hefei [8], and others from [7,9,10]. The present measurements with pure methane fuel jets give  $U_b^* = 23$ , and 29. These compare with a value of 32 from [7]. For pure propane jets, the present work gives  $U_b^* = 60$ , with values of 50 from [7] and 57 from [10].

### 3. Discussion

A simple mixing analysis demonstrates the salient aspects of the addition of air and aids understanding of the underlying influences. For non-aerated fuel jet flames there is a distribution of equivalence ratios in the flame reaction zone [3]. Remote from blow-off, computations show flame equivalence ratios close to those associated with the maximum laminar burning velocity and its maximum flame extinction stretch rate [11] This is the basis for the use of  $S_L$ , in flame height and lift-off distance correlations [6,12,13]. Both factors control the location of the flame. If the associated equivalence ratio is designated by  $\phi_m$ , then to attain it, one mole of the pure jet fuel must entrain and mix with  $[\phi_m (F/A)_s]^{-1}$  moles of atmospheric air.

For the same flow conditions, but now for one mole of an air-diluted mixture,  $(F_j + A_j)$ , but with fuel usually in excess, it was assumed that this would also entrain the same amount of atmospheric air, as the initial mixture moved towards the spatial location defined by the original  $\phi_m$  contour. Because the air entrainment and mixing processes would be very similar in the two cases, the amount of entrained atmospheric air would remain close to  $[\phi_m (F/A)_s]^{-1}$ . Hence for  $F_j$  moles of fuel with  $A_j$  moles of air in the jet, with  $F_j + A_j = 1$ , the moles of air, at the same location for the pure fuel jet  $\phi_m$  flame contour, would be  $A_j + [\phi_m (F/A)_s]^{-1}$ . The aerated jet equivalence ratio,  $\phi_a$ , at that former  $\phi_m$  contour, would now have the value:

$$\phi_a = F_j(A_j + [\phi_m (F/A)_s]^{-1})^{-1} (F/A)_s^{-1}, \quad (4)$$

with  $F_j$  and  $A_j$  given by Eq. (3). Clearly  $\phi_a < \phi_m$ . With the known values of  $(F/A)_s$ , and  $\phi_m$ , it is then possible to calculate values of  $\phi_a$  at that location, as  $A_j$  is increased. Values of  $(F/A)_s$  for stoichiometric mixtures of methane and propane are 0.105 and 0.042, respectively. In the present study, values of  $\phi_m$  were close to 1.0 for methane and 1.15 for propane.



Although this analysis tends to over-estimate the actual value of  $\phi_a$ , it is instructive to estimate from it the associated value of laminar burning velocity,  $u_a$ . Accordingly for the methane values of  $\phi_a$ , values of unstretched laminar burning velocities,  $u_a$ , were obtained from the experimental values, given as a function of equivalence ratio, in [14]. Similarly, for the propane values of  $\phi_a$  those of  $u_a$  were found from the experimental values in [15].

This approach is applied first to the methane experimental data in Fig. 5 for  $U^* = 13.2$ . The derived values of  $\phi_a$  are shown by the dashed line in Fig. 7. From these, are derived the values of the burning velocity,  $u_a$ , given by the full line curve, and in Fig. 5 by the dashed curve. Initially, there is little change in  $u_a$  with  $A_j$ , because in the regime where the burning velocity is close to its maximum value, there is little change in its value with change in equivalence ratio. However, when  $A_j$  attains a value of about 0.12,  $u_a$  begins to decrease more sharply with the changes in  $\phi_a$ .

It can be seen from Fig. 5 that, as  $A_j$  increases above 0.06, the lift-off distance increases significantly, with the flame moving downstream. At the relatively high strain rates at the location of the original  $\phi_m$  contour a flamelet only survives because its extinction stretch rate is even higher, whereas the leaner, more aerated, flame jet with a lower extinction strain rate, only survives by moving downstream, to a contour of lower mean strain rate and equivalence ratio. The increasing air dilution leads to increasing flame extinctions and instabilities. After the last measured lift-off distance there is a rapid increase in  $(L/D)f$ , followed by blow-off. The unstable transition to blow-off, occurs with  $A_j$  close to 0.21,  $\phi_a$  close to 0.77, and  $u_a = 0.22$  m/s. This point is indicated in Fig. 7 by the large diamond symbol. Bearing in mind that, in practice, the flame will be closer to extinction than is suggested by the diamond location, the methodology outlined gives a good indication of when blow-off might occur, although it cannot predict the value of  $(L/D)f$ .

The propane/air diluted jet flames of Fig. 6, are for higher values of  $A_j$ , with  $U^* = 16.2$ . With its higher value of  $(F/A)_s$ , a propane jet must entrain significantly more air than a methane jet. Values of  $\phi_a$  yielded values of  $u_a$  taken from [15]. These values decrease more sharply than those of the methane flames in Fig. 5, and this is reflected in a sharper increase in  $(L/D)f$ , up to blow-off.

In [6] values of some normalised flame surface densities in pure fuel jet flames were derived. These gave near constant values at the higher values of  $U^*$ . This is clearly not the case, as blow-off is approached, as in Figs. 3

and 4. The flame surface density could not be measured accurately, but it clearly decreases and, ultimately, vanishes.

Figure 8 summarises the measured effects of the changes in  $A_j$  on  $U_b^*$  for both fuels (including limit values for pure fuel jets), and shows the methane/air jets are more readily extinguishable. Differences in  $A_j$  for the two fuels are largely attributable to propane requiring more air to react with one mole of fuel. The presence of  $S_L$  in the expression for  $U^*$  in Eq. (1) rests upon near-stoichiometric flamelet combustion under many pure fuel jet flames practical conditions. These conditions are different in the aerated flames, where  $u_a$  is a more realistic burning velocity.

The increasingly sharp decline in  $u_a$  with increasing  $A_j$  suggests the values of  $u_a$ , appropriate to  $A_j$  might be inserted in place of  $S_L$  and also where it appears in the expression for  $\delta$ , within the expression for  $U^*$  in Eq. (1). Relationships, such as those between  $u_a$  and  $A_j$  in Figs. 5 and 6, provide the appropriate values of  $u_a$  in now, differently defined, values of  $U_b^*$ , based on  $u_a$  and indicated by  $U_{ba}^*$ . These are shown by the broken straight lines for both methane and propane in Fig. 8. As  $U_b^*$  declines, the increasingly lean combustion at low extinction stretch rates will increase emissions of unburned hydrocarbons prior to blow-off.

Concerning the generality of the analytical approach adopted, it might also be argued, with regard to the correlation with  $A_j$  in Fig. 8, that the amount of added air should more rationally be related to that required to burn one mole of fuel, and, consequently,  $A_j$  should be multiplied by the  $(F/A)_s$  value, appropriate to each fuel. This approach is adopted in Fig. 9, which shows plots of  $U_b^*/U_{bo}^*$  against  $A_j(F/A)_s$ , where  $U_{bo}^* = U_b^*$  at  $A_j = 0$  for each fuel, as well as of  $U_{ba}^*/U_{bo}^*$ . It can be seen that  $A_j(F/A)_s$  provides a more compact and rational correlation, and brings the methane and propane results into a similar regime. There is a greater spread between  $U_{ba}^*/U_{bo}^*$  and  $U_b^*/U_{bo}^*$  values for propane, because of the greater spread of  $S_L$  and  $u_a$  values than for methane.

#### 4. Conclusions

1. Whereas, with normal subsonic fuel jet combustion, very high jet velocities are required to demonstrate flame extinction effects that lead to blow-off, these effects become more clearly demonstrated with added air at lower flow rates.
2. Unlike flame lift-off distances, it is difficult to generalise the conditions for jet flame blow-off, which are unique to each fuel.
3. Partly because flame instabilities develop prior to blow-off, different methods of estimating it have been employed. The present work employs the highest stable value of  $U^*$  prior to blow-off. This gives values for

pure fuel jets of 25 for methane and 60 for propane. These compare with measured values of 32 and 50, respectively, in [7], for similar conditions.

4. The earlier onset of blow-off by added air has been measured and is explained, by a simplified mixing theory, in terms of the leaning-off of the reaction zone and reductions in burning velocity and the flame extinction stretch rates of the flamelets.
5. Experiments with added air have improved understanding of fuel jet combustion. Initially, this air might enhance the attainment of a mixture with a near maximum burning velocity mixture, but with increasing jet velocity and air entrainment, the leaner flame moves downstream with an increasing flame lift-off distance, followed by blow-off.
6. Propane flames are more tolerant of added air, due to the larger amount of air required per mole of propane than of methane.
7. The decline in  $U_b^*$  with increasing  $A_j$  is due to the reduction in flamelet burning velocities and their flame extinction stretch rates.
8. As  $U_b^*$  declines in value with increasing air dilution, the emission of unburned hydrocarbons will increase prior to blow-off.
9. The more compact regime for both fuels, when expressed in terms of  $A_j(F/A)_s$ , demonstrates the role of the required amount of air in jet flames, just as the greater differences between  $U_{ba}^*/U_{bo}^*$  and  $U_b^*/U_{bo}^*$  for propane and methane demonstrate the roles of both air dilution and  $u_a$ .

### **Acknowledgments**

A.P. gratefully acknowledges financial support of the Royal Society, in the form of a Postdoctoral Newton International Fellowship.

### **References**

- [1] Johnson MR, Kostiuk LW. A parametric model for the efficiency of a flame in crosswind. Proc. Combust. Inst 2002;29:1943-50.
- [2] Bradley D, Gaskell PH, Lau AKC. A mixedness-reactedness flamelet model for turbulent diffusion flames. Proc. Combust. Inst 1991;23:685-92.
- [3] Bradley D, Gaskell PH, Gu XJ. The mathematical modeling of liftoff and blowoff of turbulent non-premixed methane jet flames at high strain rates. Proc. Combust. Inst 1998; 27:1199-1206.

- [4] Bradley D, Emerson DR, Gaskell PH, Gu XJ. Mathematical modelling of turbulent non-premixed piloted-jet flames with local extinctions. *Proc. Combust. Inst* 2002; 29:2155-62.
- [5] Chen Z, Ruan S, Swaminathan N. Simulation of turbulent lifted methane jet flames: effects of air-dilution and transient flame propagation. *Combust. Flame* 2015;162:703-16.
- [6] Bradley D, Gaskell PH, Gu XJ, Palacios A. Jet flame heights, lift-off distances and mean flame surface density for extensive ranges of fuels and flow rates. *Combust. Flame* 2016;164:400-9.
- [7] Kalghatgi GT. Blow-out stability of gaseous jet diffusion flames. Part I: in still air. *Combust. Sci. Technol* 1981;26:233-9.
- [8] Palacios A, Bradley D, Lawes M. Blow-off velocities of jet flames. In: Chao J, Molkov V, Sunderland P, Tamanini F, Torero J, editors. *Proceedings of the Eighth International Seminar on Fire and Explosion Hazards*, Hefei, China: University of Science and Technology of China; 2016.
- [9] Hu L, Zhang X, Wang Q, Palacios A. Flame size and volumetric heat release rate of turbulent buoyant jet diffusion flames in normal- and a sub-atmospheric pressure. *Fuel* 2015;150:278-87.
- [10] Palacios A, Muñoz M, Casal J. Jet fires: an experimental study of the main geometrical features of the flame in subsonic and sonic regimes. *AIChE J* 2009;55:256-63.
- [11] Bradley D. *Fundamentals of Lean Combustion*. In: Dunn-Rankin D, editor. *Lean Combustion Technology and Control*, Burlington MA, USA: Academic Press; 2008, p. 19-53.
- [12] Vanquickenborne L, Van Tiggelen A. The stabilization mechanism of lifted diffusion flames. *Combust. Flame* 1966;10:59-69.
- [13] Kalghatgi GT. Lift-off heights and visible lengths of vertical turbulent jet diffusion flames in still air. *Combust. Sci. Technol* 1984;41:17-29.
- [14] Gu XJ, Haq MZ, Lawes M, Wooley R. Laminar burning velocity and Markstein lengths of methane-air mixtures. *Combust. Flame* 2000;121:41-58.
- [15] Bosschaart KJ, De Goey LPH. The laminar burning velocity of flames propagating in mixtures of hydrocarbons and air measured with the heat flux method. *Combust. Flame* 2004;136:261-9.

## List of Figure Captions

Figure 1. Computed radial and axial variations of flow streamlines (dotted) and volumetric heat release rate (full contours), of methane jet flame.  $D = 9$  mm ( $r = 4.5$  mm), all distances in mm. From [3].

Figure 2. Normalised flame lift-off distances for methane and propane subsonic fuel jets. Modified from [6], involving only methane and propane as fuels. Methane data indicated by open symbols. Location of blow-off values indicated by arrows.

Figure 3. Oscillatory methane jet flame images prior to blow-off, at fixed subsonic flow on a 3 mm diameter pipe. Flow rates 10.24 L/min of  $\text{CH}_4$  and 3 L/min of air, and values of  $A_j = 0.227$  and  $U_b^* = 14.4$ . Time interval between successive images is 3 s.

Figure 4. Oscillatory aerated methane jet flame with values of  $A_j = 0.156$  and  $U_b^* = 10.3$  prior to blow-off. Lift-off distances leading up to blow-off. Time interval between successive data points is 0.25 s.

Figure 5. Measured lift-off ( $L/D$ )<sub>f</sub> for methane jet as a function of the mole fraction of jet air,  $A_j$ .

Figure 6. Measured lift-off ( $L/D$ )<sub>f</sub> for propane jet as a function of the mole fraction of jet air,  $A_j$ .

Figure 7. Effect of increasing jet air dilution on  $\phi_a$ , and laminar burning velocity,  $u_a$ , of  $\text{CH}_4/\text{air}$ , for conditions of Fig. 5. Filled diamond symbol indicates estimated onset of blow-off.

Figure 8. Blow-off  $U_b^*$  for methane/air and propane/air: variation with mole fraction of air in jet gas. Broken lines show  $U_{ba}^*$ .

Figure 9. Broken lines show values of  $U_{ba}^*/U_{bo}^*$ , X indicates propane/air, and O methane/air, mixtures.

Table 1

Range of values in present experiments (including those of Fig. 2).

Fuel	Gas exit velocity, $u_1$ , m·s <sup>-1</sup>	Initial stagnation pressure, $P_i$ , MPa	Pipe diameter, $D$ , mm
CH <sub>4</sub>	9-448	0.1-0.11	1-51
C <sub>3</sub> H <sub>8</sub>	5-249	0.1-0.11	0.84-43.1
CH <sub>4</sub> /air	16-63	0.1-0.11	3-4
C <sub>3</sub> H <sub>8</sub> /air	25-221	0.1-0.11	3-8

Table 2

Conditions for blow-off for separate dilution with air of methane and propane.

Methane $S_L = 0.36$ m/s $(F/A)_s = 0.105$						Propane $S_L = 0.475$ m/s $(F/A)_s = 0.042$					
$A_j$	$u$ , m/s	$D$ , mm	$u_a$ , m/s	$P_i$ , MPa	$U_b^*$	$A_j$	$u$ , m/s	$D$ , mm	$u_a$ , m/s	$P_i$ , MPa	$U_b^*$
0	62.9	3	0.36	0.19	29.0	0	221	8	0.475	0.18	60.0
0.02	55.3	4	0.36	0.19	22.7	0.02	215.4	8	0.475	0.18	59.8
0.05	54.7	4	0.36	0.19	22.5	0.05	189.1	6	0.475	0.18	59.0
0.238	24.1	3	0.2	0.19	14.6	0.468	45.5	3	0.14	0.18	18.9
0.25	21.2	3	0.2	0.19	13.1	0.569	31.6	4	0.09	0.18	11.7
0.266	18.9	3	0.175	0.19	11.9	0.656	25.3	5	0.07	0.18	8.56
0.294	16.5	3	0.16	0.19	10.8						

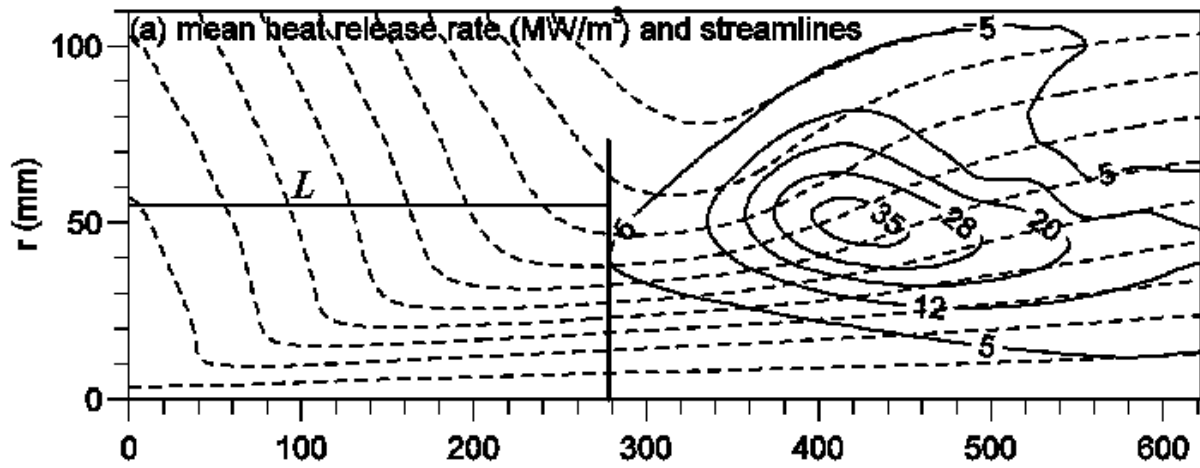


Figure 1. Computed radial and axial variations of flow streamlines (dotted) and volumetric heat release rate (full contours), of methane jet flame.  $D = 9 \text{ mm}$  ( $r = 4.5 \text{ mm}$ ), all distances in mm. From [3].

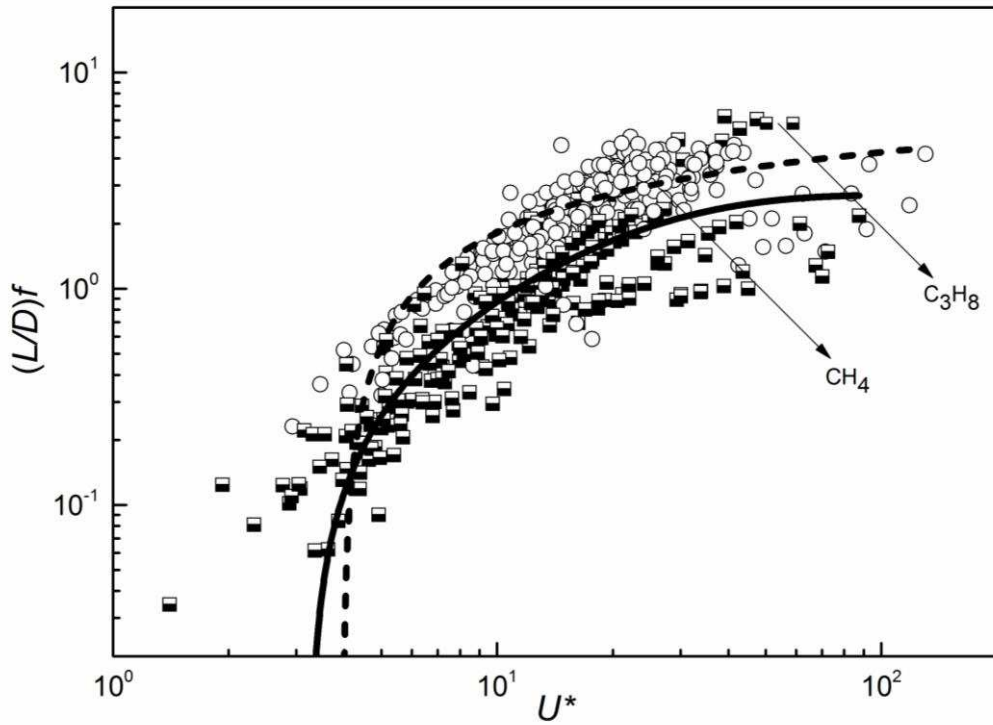


Figure 2. Normalised flame lift-off distances for methane and propane subsonic fuel jets. Modified from [6], involving only methane and propane as fuels. Methane data indicated by open symbols. Location of blow-off values indicated by arrows.

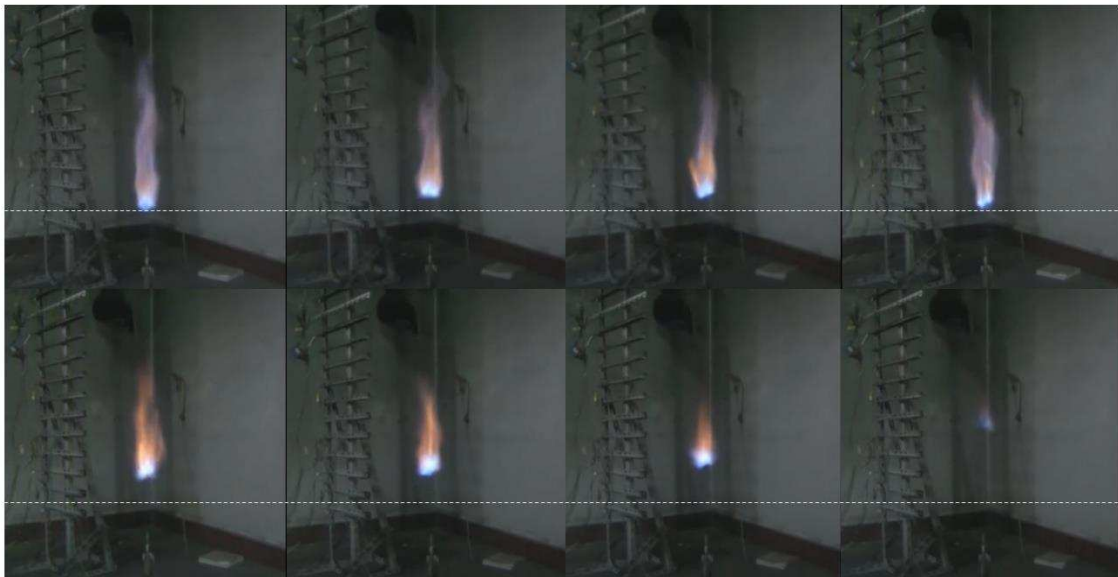


Figure 3. Oscillatory methane jet flame images prior to blow-off, at fixed subsonic flow on a 3 mm diameter pipe. Flow rates 10.24 L/min of  $\text{CH}_4$  and 3 L/min of air, and values of  $A_j = 0.227$  and  $U_b^* = 14.4$ . Time interval between successive images is 3 s.



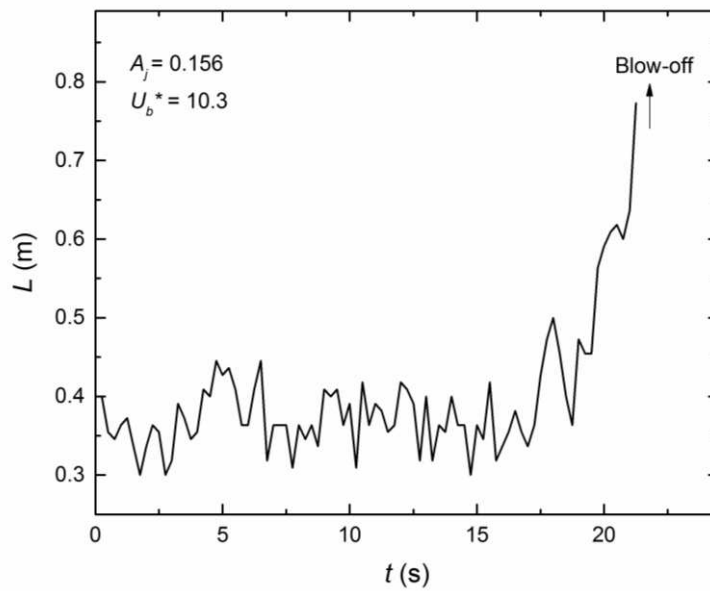


Figure 4. Oscillatory aerated methane jet flame with values of  $A_j = 0.156$  and  $U_b^* = 10.3$  prior to blow-off. Lift-off distances leading up to blow-off. Time interval between successive data points is 0.25 s.

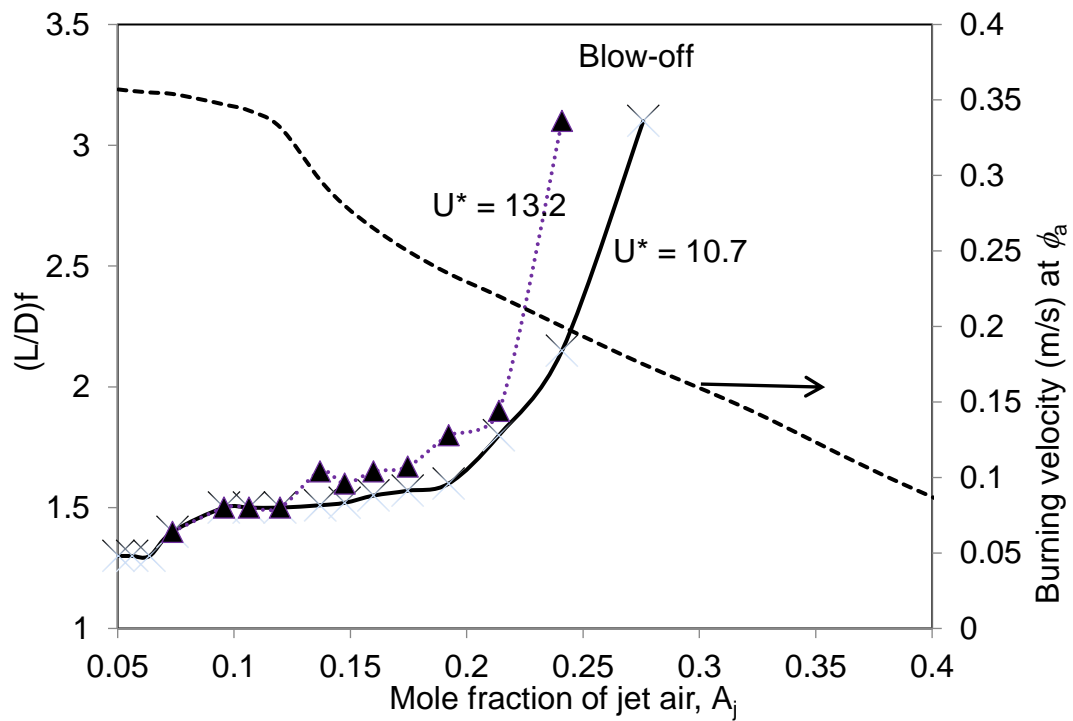


Figure 5. Measured lift-off  $(L/D)f$  for methane jet as a function of the mole fraction of jet air,  $A_j$ .

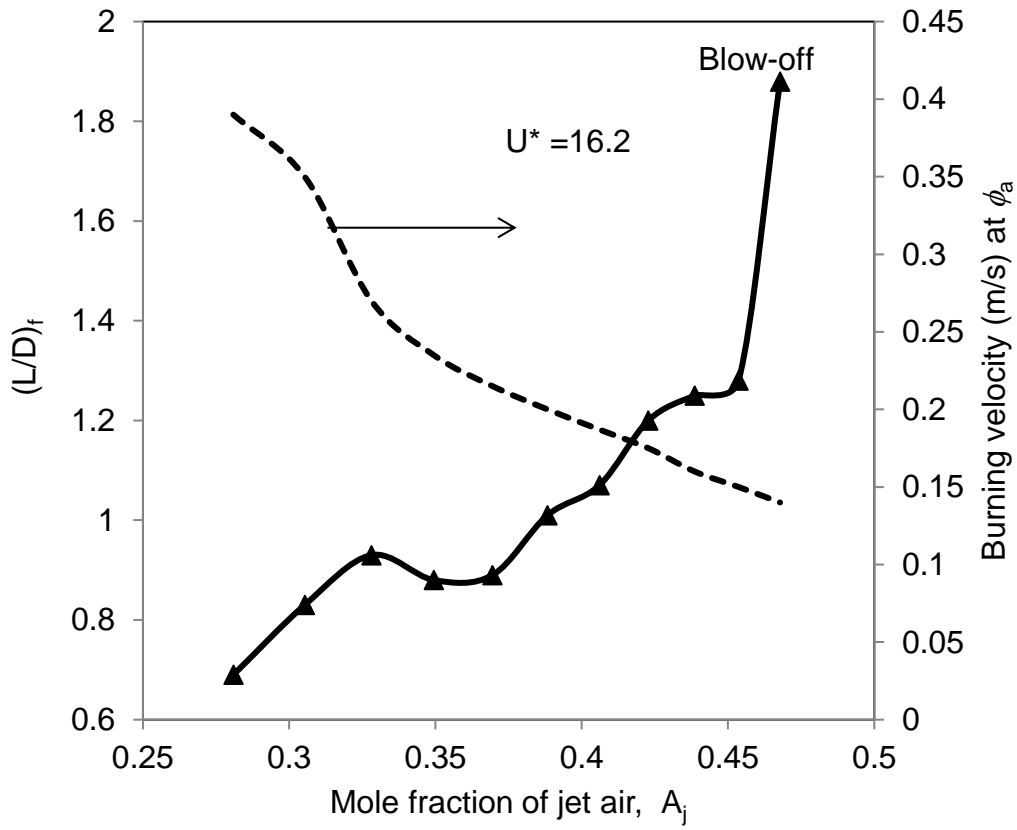


Figure 6. Measured lift-off  $(L/D)_f$  for propane jet as a function of the mole fraction of jet air,  $A_j$ .

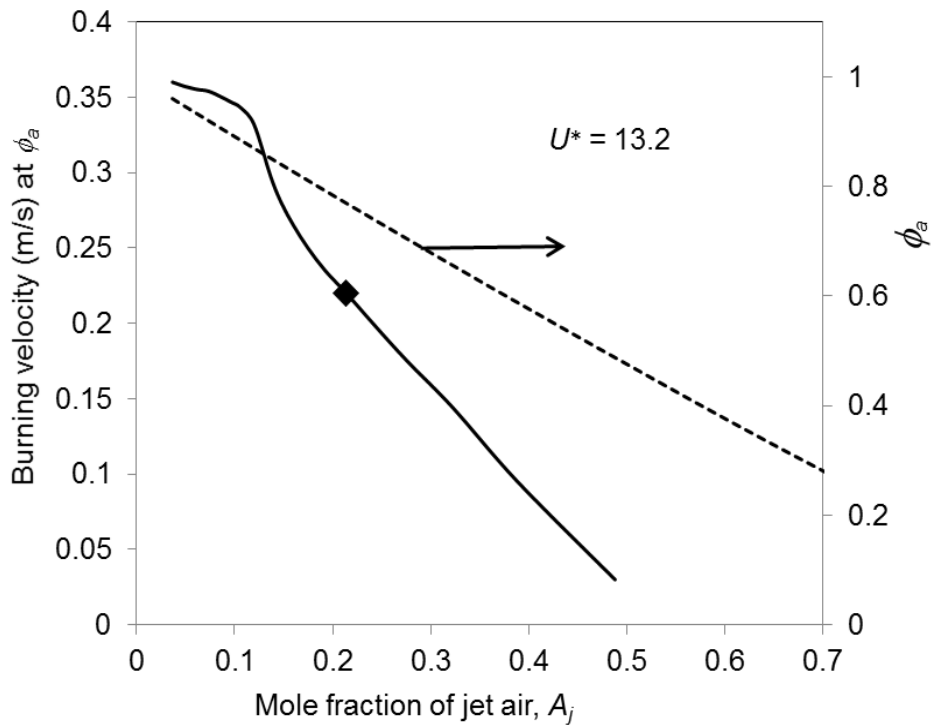


Figure 7. Effect of increasing jet air dilution on  $\phi_a$ , and laminar burning velocity,  $u_a$ , of  $\text{CH}_4/\text{air}$ , for conditions of Fig.

5. Filled diamond symbol indicates estimated onset of blow-off.

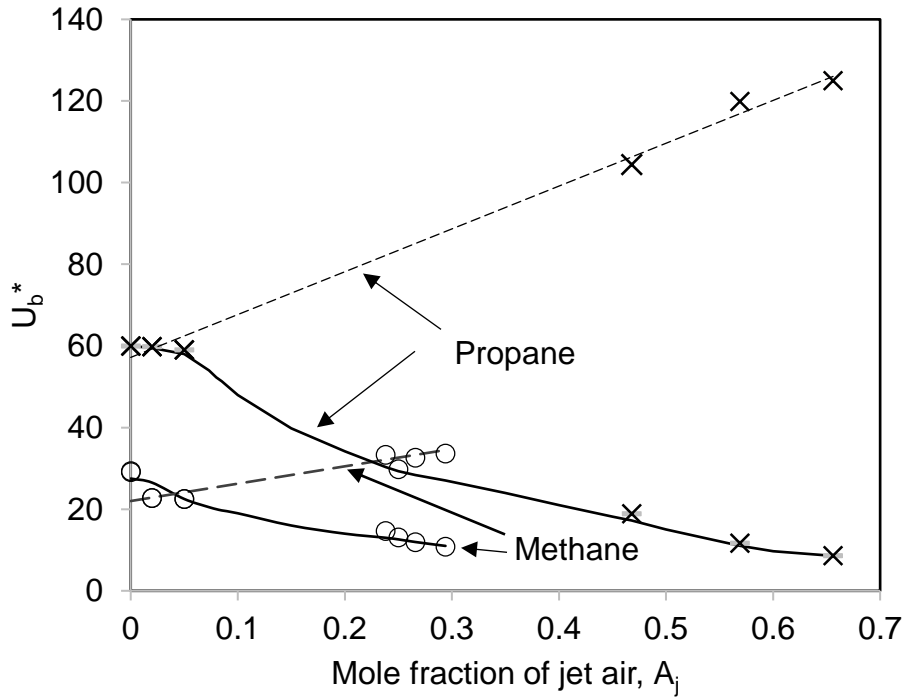


Figure 8. Blow-off  $U_b^*$  for methane/air and propane/air: variation with mole fraction of air in jet gas. Broken lines show  $U_{ba}^*$ .

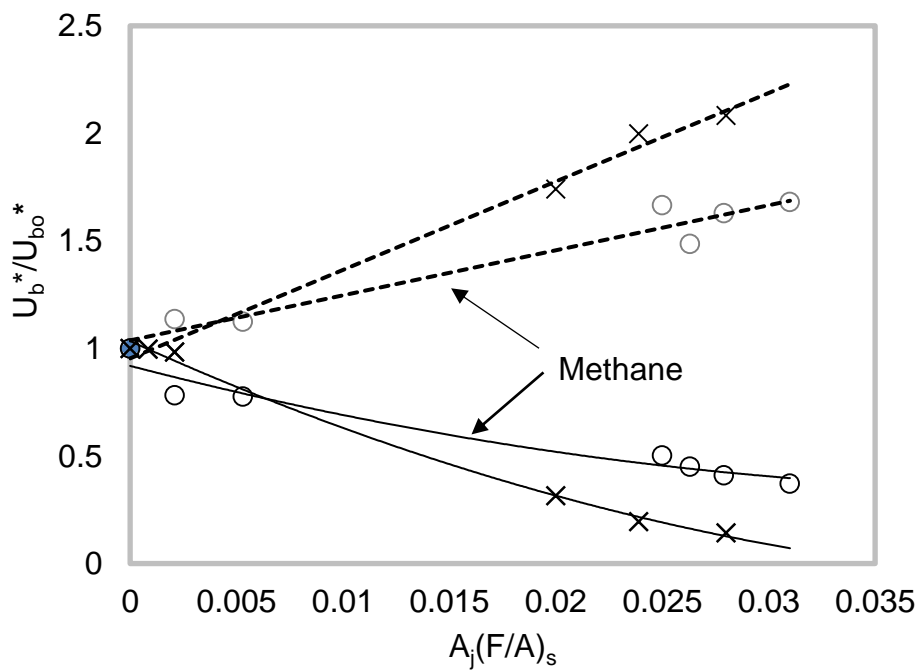


Figure 9. Broken lines show values of  $U_{ba}^*/U_{bo}^*$ , X indicates propane/air, and O methane/air, mixtures.